Surface anchoring effect on the morphology and performance of polymer-dispersed liquid crystal

Yi-Hsin Lin, Hongwen Ren, Yung-Hsun Wu, Xiao Liang and Shin-Tson Wu

College of Optics and Photonics, University of Central Florida, Orlando, FL 32816

Abstract

Surface effects on the phase separation dynamics, morphologies, and electro-optic properties of thin polymer-dispersed liquid crystal (PDLC) cells are investigated. Four types of surface alignment layers were studied: ITO only, Polyimide (PI) without rubbing, homogeneous cell, and 90° twisted nematic (TN) cell. The ITO-only and non-rubbed PI cells do not provide enough anchoring force to prevent LC droplets flow and coalesce. As a result, the droplets are larger and less uniform. For the homogeneous and TN cells with sufficiently high anchoring energy, almost all the nucleated LC droplets grow at a fixed position during phase separation. The appearance of the coalescence is not obvious and the formed LC droplets are relatively uniform. For the rubbed cells with polar anchoring energy $>2\times 10^{-4}$ J/m^2, the droplet size is smaller and more uniform than those in the conventional PDLC cell. The phase separation dynamics determine the final composite morphology which affects the electro-optic properties of a PDLC device. The morphologies in the homogeneous and TN cells are similar, but the TN cell is polarization independent while the homogeneous cell is polarization dependent. Moreover, the TN PDLC cell exhibits a higher contrast ratio. The light shutter made of TN PDLC shows no haze and 5-10 ms response time.

Keywords: polymer-dispersed liquid crystal, surface anchoring effect, morphologies, high contrast ratio.

1. INTRODUCTION

Polymer dispersed liquid crystals (PDLCs), consisting of micron-sized LC droplets dispersed in a polymer matrix, are a promising electro-optic material for displays [1,2], light switches [3-8] and tunable-focus lenses [9] because of their polarization independence. The phase separation, which is an important process affecting the electro-optic properties of PDLCs, has been studied by computer simulations [10-13] and by experiments [14,15]. In a conventional PDLC, the formed droplets, each about the size of a visible wavelength, are randomly distributed in the polymer matrix. Typically, the LC and monomer mixture is sandwiched between two indium-tin-oxide (ITO) glasses without any surface treatments. After photo-induced phase separation, the droplets are formed and their sizes vary. Due to the relatively large cell gap and micron-sized LC droplets, phase separation dynamics do not depend on surface interaction. The phase separation dynamics determine the final composite morphology of PDLC. The more uniform LC droplets exhibit a higher light scattering efficiency and higher device contrast ratio [16,17].

Several factors, such as the transition from isotropic to nematic ordering of the LCs, the solubility of the LC and monomer, the growing molecular weight and the gelation of polymer matrix and elastic forces in the polymer matrix [16,18], compete with each other to determine the phase separation dynamics of PDLCs. In this Letter, we demonstrate that the phase separation dynamics are influenced by the surface effect for a PDLC confined in a thin cell. The PDLCs with a strong surface anchoring exhibit smaller LC droplets and better uniformity because the anchoring force in the boundaries fixes the droplets and prevents them from flowing and coalescing.

2. SAMPLE PREPARATION

To fabricate a PDLC device, we mixed UV-curable monomer NOA65 in a nematic LC host (E48, $\Delta n = 0.231$ at $\lambda = 589$ nm and $T = 22^{\circ}C$). We varied the polymer concentration from 20 to 40 wt%. However,

Emerging Liquid Crystal Technologies, edited by Liang-Chy Chien,
Proceedings of SPIE Vol. 5741 (SPIE, Bellingham, WA, 2005)
0277-786X/05/$15 · doi: 10.1117/12.590405

the general phenomena remain the same except for the different droplet sizes. Thus, we focus our discussions using the PDLC with 30 wt% NOA65 as examples. The LC and monomer mixture was injected into an empty cell in the isotropic state. The cell gap is d=8 μm. For comparison, we prepared several types of cells with different surface treatments: 1) a conventional PDLC cell, i.e. the indium-tin-oxide (ITO) glass substrates without polyimide (PI) alignment layers, 2) a PI cell, i.e. an ITO glass cell with each inner surface overcoated with a thin (~10 nm) PI layer but without rubbing, 3) a 90° twisted nematic (TN) cell, i.e. the ITO glass substrates with orthogonal rubbing alignment layers, 4) a homogeneous cell, i.e. the ITO glass substrates with anti-parallel rubbing alignment layers, 5) a 45° twisted nematic (45°-TN) cell, i.e. the rubbing directions of the ITO glass substrates are at 45°, and 6) a single-sided rubbing cell, in which only one substrate was rubbed, the other had plain PI. In the TN and homogeneous cells, the polar anchoring energy of the buffed PI layers was measured to be ~$3x10^{-4}$ J/m^2 by the voltage-dependent phase retardation method [19,20]. The pretilt angle of these cells is about 3°.

3. EXPERIMENTAL RESULTS

Figures 1(a) to 1(f) show the morphologies of the abovementioned UV-cured PDLC cells observed from a polarized optical microscope in the voltage-off state. The UV exposure intensity was I=60 mW/cm^2 and the curing time for both cells was 15 min at T=20 °C. From Figs. 1(a) and 1(b), we find that the LC droplets in the conventional and non-rubbed PI cells are larger and less uniform than those observed in Fig. 1(d) for the 90°-TN cells, Fig. 1(e) for the 45°-TN cells and Fig. 1(f) for the homogeneous cells. That means the rubbed PI surfaces have a crucial influence on the phase separation of PDLC when the cell gap is thin. The smaller and more uniform LC droplets exhibit a higher light scattering efficiency which, in turn, leads to a higher device contrast ratio. [17] The droplets are more uniform in the single-sided rubbing than in the conventional and non-rubbed PI cells. Besides, the single-sided rubbing has larger droplet sizes than the TN, 45°-TN and homogeneous cells. For comparison, the morphologies of a weak-rubbing homogeneous cell (Fig. 1(g); anchoring energy W~$1x10^{-4}$ J/m^2) and sputtered SiO_2 alignment layers (Fig. 1(h); W~$8x10^{-5}$ J/m^2) are also less uniform.

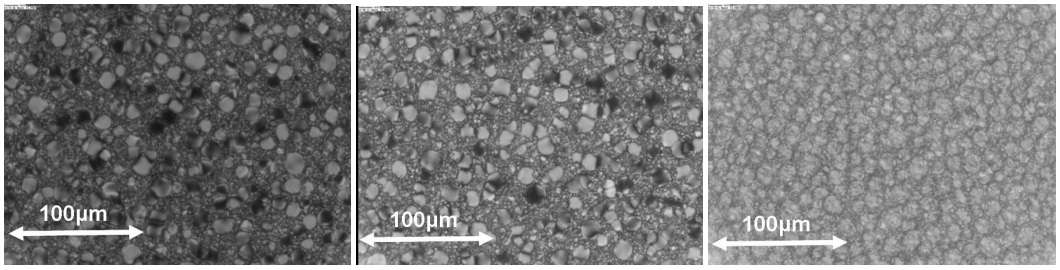

(a) (b) (c)

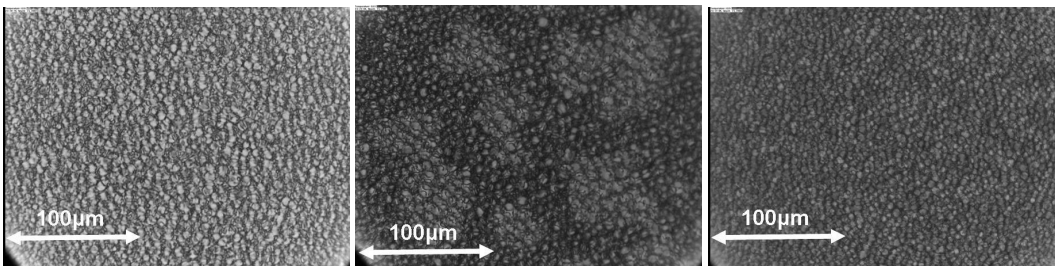

(d) (e) (f)

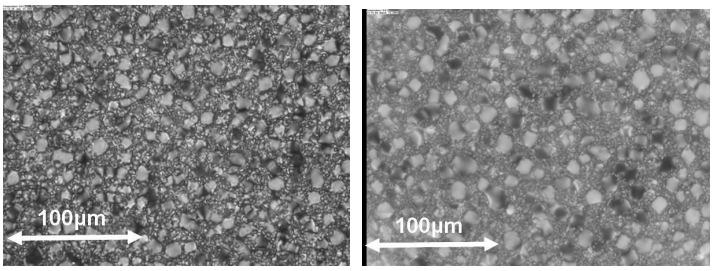

(g) (h)

Fig. 1. Phase separation morphologies of PDLC in (a) conventional cell, (b) PI cell without rubbing, (c) single-side rubbing (d) 90°-TN cell (anchoring energy $W\sim3\times10^{-4}$ J/m^2), (e) 45°-TN cell ($W\sim3\times10^{-4}$ J/m^2), (f) homogeneous cell ($W\sim3\times10^{-4}$ J/m^2), (g) homogeneous cell (weak rubbing, $W\sim1\times10^{-4}$ J/m^2), and (h) homogeneous cell with SiO_2 alignment layers ($W\sim8\times10^{-5}$ J/m^2) observed from a polarized optical microscope. LC/monomer mixture: 70 wt% E48 and 30 wt% NOA65. All the devices have the same cell gap d~8 μm.

To show that the phase separation dynamics indeed depend on the surface rubbing conditions, we observed the morphologies of the four PDLC cells from a polarized optical microscope in the voltage-off state before UV curing. Results are shown in Figs. 2(a)-(d). The cells were put on a heating stage and their temperatures were probed by a thermocouple. In Figs. 2(a) and 2(b), the LC droplets in the conventional substrates and in the PI cells start to appear at T~40 °C when the temperature was cooled from the clearing point (T_c=65 °C) of the LC/monomer mixture. In both figures, the LC droplets nucleate and grow at the beginning and then rapidly flow and coalesce due to the absence of the anchoring force (for the conventional cell) or a weak anchoring force (for the PI cell) in the ITO substrates during the cooling process. In Figs. 2(c) and 2(d), the LC droplets confined in the TN and homogeneous cells begin to appear at T~38 °C when the temperature is cooled down slowly from T_c=65 °C. The LC droplets continue to nucleate and grow but remain basically static during the cooling process. These droplets move only slightly but barely coalesce with the surrounding droplets. This is because the strong anchoring forces from the boundaries prevent the LC droplets from flowing. As the temperature decreases, the sizes of the LC droplets in both of the rubbed cells are smaller and the size variation is less than those in the non-rubbed PI cells. The color difference between the low and high temperatures is due to the temperature-dependent LC birefringence. [21]

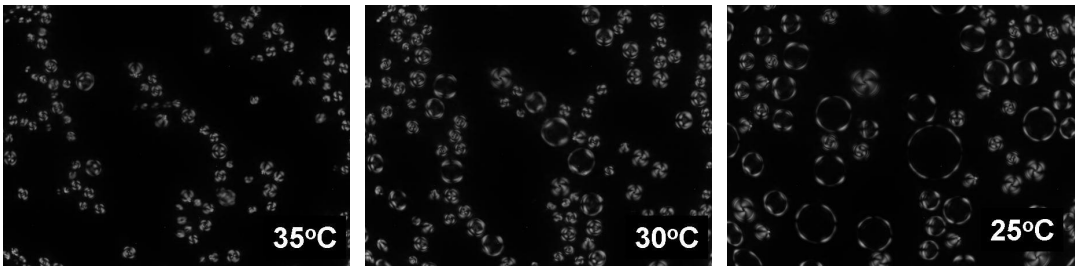

(a)

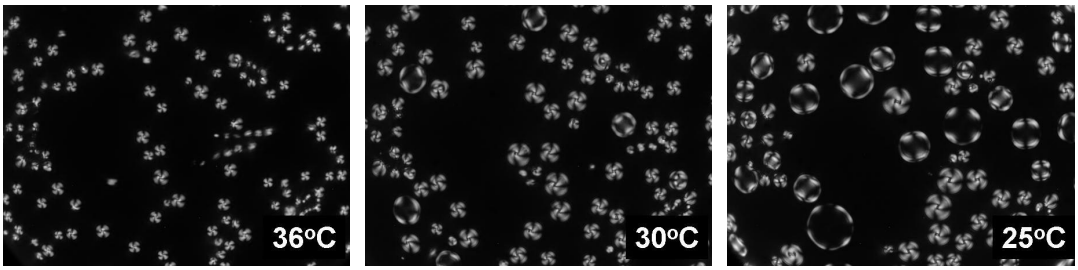

(b)

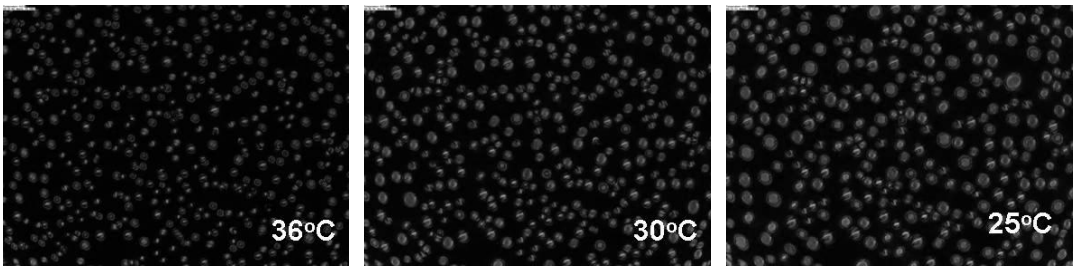

(c)

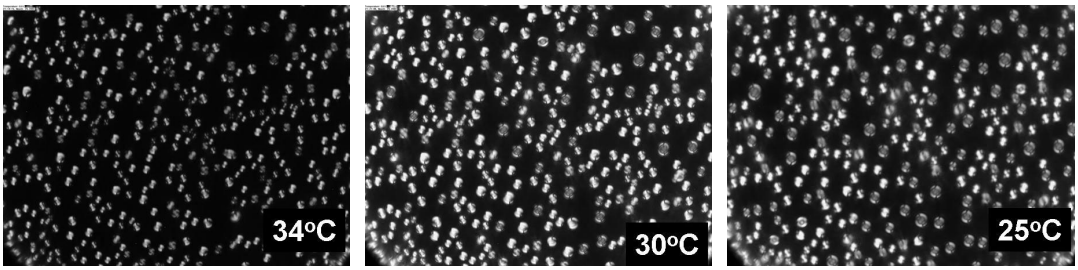

(d)

Fig. 2 The dynamic phase separation morphologies of PDLC observed from a polarized optical microscope under different temperatures without UV illumination: (a) conventional PDLC cell, (b) PI without rubbing, (c) TN cell, and (d) homogeneous cell.

In Figs. 3 and 4, the cells were cooled to T=27°C and then illuminated by UV light at t=0. Meanwhile, the phase separation animations were simultaneously recorded on a digital camera (Olympus Camedia C-3040) connected to a polarized optical microscope. In Figs. 3(a)-(b), we show the time-resolved morphologies in the conventional cell (without PI) and the PI cell without rubbing. The LC droplets exist at t=0 due to the thermal-induced phase separation even before UV exposure took place. The following nucleated LC droplets caused by the increased expulsion of LCs from the polymer matrix flow in the conventional and PI cells due to the weak or the lack of anchoring forces in the boundary substrates. When the nucleated and flowing LC droplets approach each other, they coalesce. As the polymerization reaction continues, gelation gradually occurs which resists the growth of the moving and nucleating LC droplets. The LC droplets are frozen by the polymer matrix when the polymer matrix reaches its gelation point. The morphologies remain basically unchanged after t=6 s for the conventional cell and after t=5 s for the PI cell without rubbing because the polymer matrix has either grown sufficiently in molecular weight or reached its gelation point, impeding further coalescence. The resultant morphology consists of LC droplets dispersed in the polymer matrix. The droplet size decreases with an increase in the UV curing temperature

or UV exposure intensity. The sizes of the LC droplets are not quite uniform due to first the flow and then the coalescence.

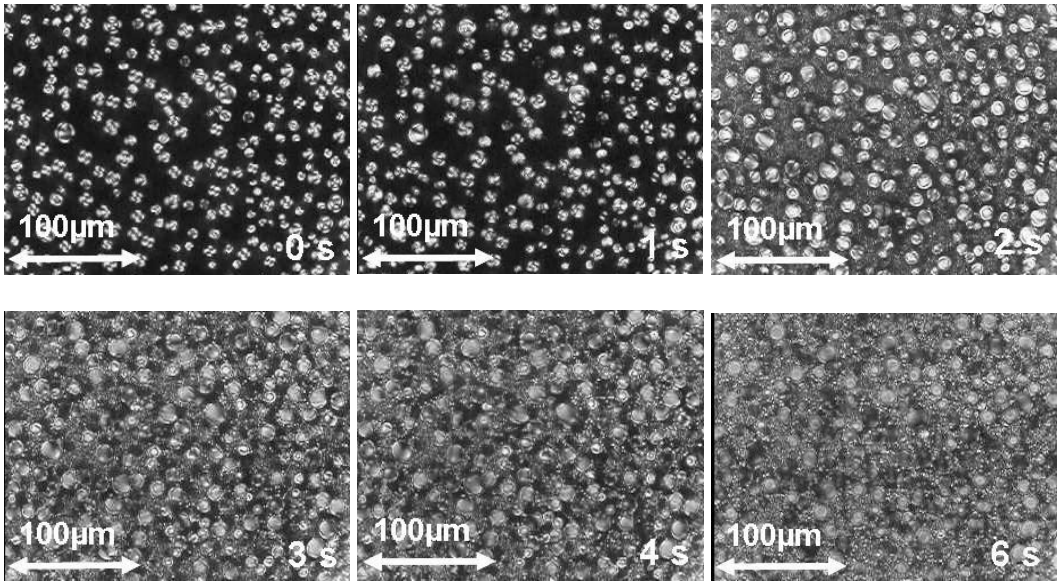

(a)

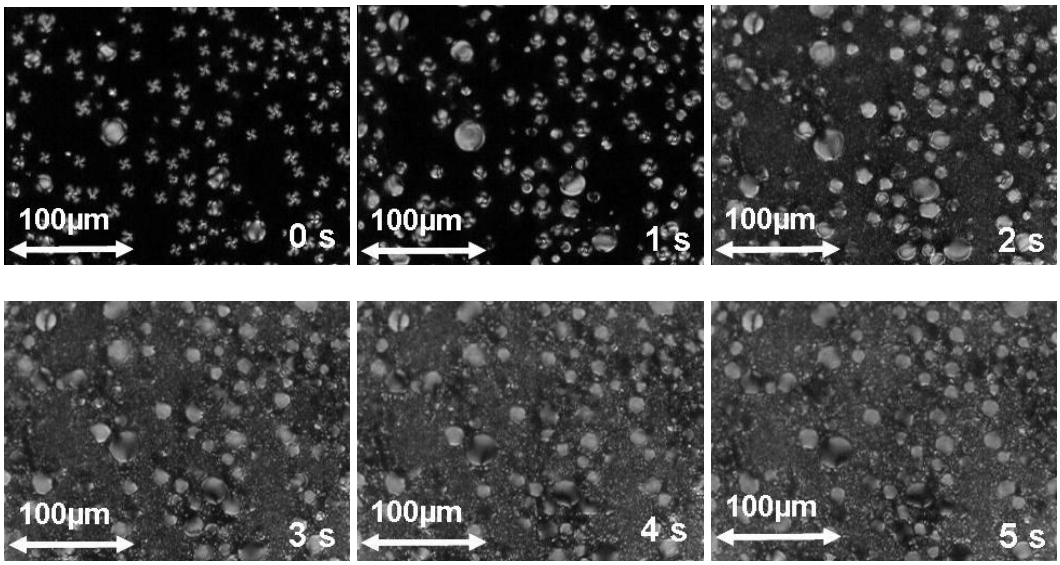

(b)

Fig. 3 The dynamic phase separation morphologies of PDLC at T=27°C with UV exposure starting at t=0: (a) conventional cell without PI, and (b) PI cell without rubbing. The UV intensity is I=60 mw/cm^2.

The time-resolved morphologies in the TN and homogeneous cells are shown in Figs. 4(a) and 4(b), respectively. The cells were also cooled to T=27°C and illuminated by UV light at t=0. At t=0, the morphologies shown in Figs. 4(a) and 4(b) are different from those shown in Figs. 3(a) and 3(b). The LC droplets appear to be smaller in size and are uniformly dispersed at t=0 because they are anchored by the boundary anchoring force which prevents the droplets from moving and coalescing. As the photo-induced polymerization reaction goes on, the LC droplets are frozen by the boundary anchoring force and by the polymer matrix which gradually reaches its gelation point. The LC droplets stop growing when the gelation

point of the polymer matrix is reached. The morphologies which have better uniformity and smaller droplet sizes remain the same after 4 seconds in the TN and homogeneous cells.

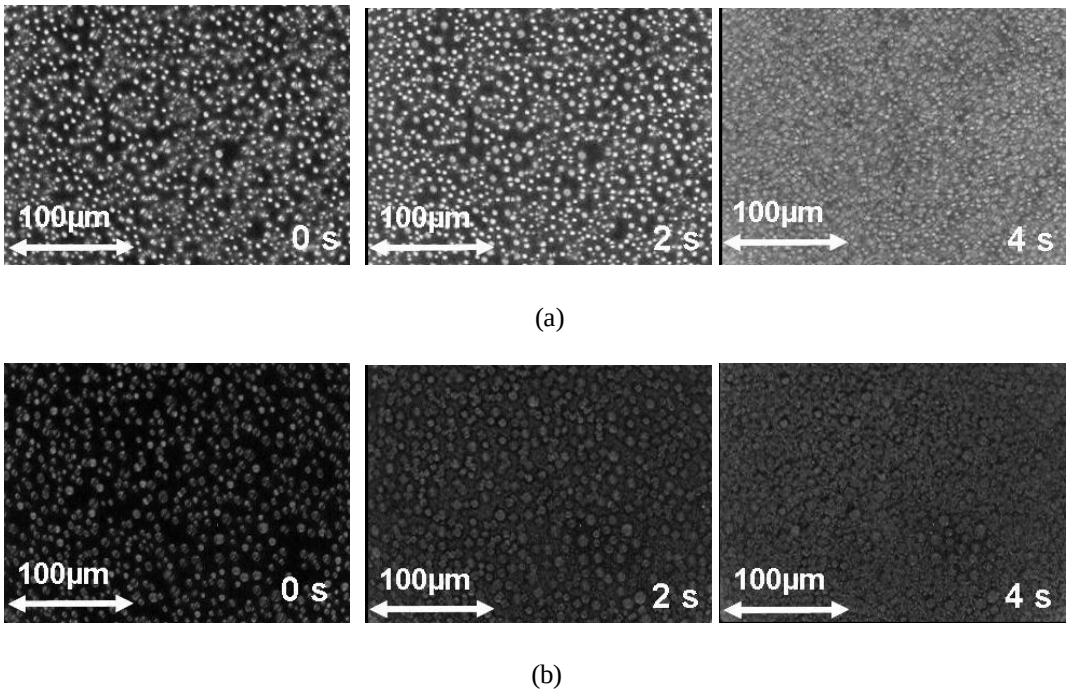

Fig. 4 The dynamic phase separation morphologies of PDLC at T=27°C with UV exposure starting at t=0: (a) TN cell, and (b) homogeneous cell. The UV intensity is I=60 mw/cm^2 and cell gap d=8 μm.

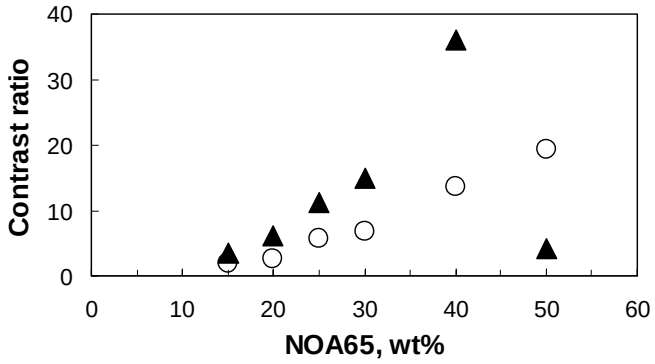

Fig. 5 Polymer concentration effect on device contrast ratio. Triangles are for the 6.5 μm TN-PDLC cell and circles are for the 8 μm conventional PDLC cell.

The electro-optic properties of the PDLC and TN-PDLC cells were studied by measuring the transmittance of an unpolarized He-Ne laser beam (λ=633 nm) at normal incidence. The photodiode detector was placed at ~20 cm behind the sample; the corresponding collection angle is ±1°. The voltage dependent transmittance curves were recorded by the LabVIEW data acquisition system. The response time was measured using a digital phosphor oscilloscope. To evaluate the contrast ratios of the TN-PDLC and PDLC cells, we measured their voltage-dependent transmittance. To calibrate the substrate reflection losses, the transmittance of a homogeneous cell filled with E48 LC mixture is defined as unity. In a TN-PDLC cell,

the LC molecules inside the droplets near the substrates present orthogonal orientation. In the bulk, the LC droplets are randomly distributed. Therefore, its light scattering behavior in the voltage-off state is also independent of polarization, similar to a conventional PDLC. In the low voltage regime, the TN-PDLC cell exhibits a better dark state than conventional PDLC cell. The saturation voltage of both cells occurs at ~20 V_{rms}. Thus, we compare the contrast ratio at V= 20 V_{rms}, i.e. $CR = T(V = 20)/T(V = 0)$. Figure 5 shows the polymer concentration dependent contrast ratio (measured at V=20 V_{rms}) for TN-PDLC (triangles) and conventional PDLC (circles).We have varied the polymer concentration from 15% to 50%. In both TN-PDLC and conventional PDLC cells, the droplet size decreases as the polymer concentration increases. In the same polymer concentration, the droplet size of TN-PDLC is roughly ~1.5X smaller than that of conventional PDLC. Therefore, the optimal polymer concentration for maximizing light scattering (i.e. droplet size is comparable to the laser wavelength) for TN-PDLC and conventional PDLC is different. For TN-PDLC, the optimal polymer concentration would be lower than that for conventional PDLC.

From Fig. 5, as the polymer concentration increases, the contrast ratios for both T-PDLC and PDLC cells increase almost linearly but at different slopes. For the 6.5-μm TN-PDLC, the optimal polymer concentration occurs at c~40% where the contrast ratio reaches ~35:1. At c=50%, the droplet size becomes much smaller than the He-Ne laser wavelength. Moreover, the influence of surface anchoring to these tiny droplets is no longer significant. As a result, the contrast ratio decreases sharply. On the other hand, for the 8-μm conventional PDLC at c=50% its droplet size is still ~1.5X larger than that of TN-PDLC so that the light scattering remains significant. Its optimal polymer concentration should occur at a higher level. Increasing cell gap would improve the contrast ratio for both TN-PDLC and conventional PDLC at the expense of increased voltage. Increasing curing temperature[10] is another option for improving contrast ratio. However, the response time becomes slower.

The response time of the transmissive TN-PDLC and PDLC cells was measured at room temperature using 20 V_{rms} square pulses. In general, the PDLC response time depends on the LC viscosity, droplet size and shape, and the ratio of the applied voltage over threshold voltage For the 6.5-μm-thick TN-PDLC cell (c=40%), the measured rise time (10-90%) is ~5 ms and decay time (90-10%) is ~10 ms. In contrast, the 40% conventional PDLC has 7.6 ms rise time and 21 ms decay time. The faster response time of TN-PDLC originates from its smaller droplet sizes. To further improve switching speed, we could reduce the droplet size by increasing the polymer concentration or use a lower viscosity LC. However, smaller droplet sizes require a higher operating voltage. Holographic PDLC is such an example.

Figure 6 shows the morphologies of homogeneous PDLC cells with various cell gaps at T=20°C, as observed from a polarized optical microscope. The larger cell gap shows a larger droplet size. This is because the strong boundary effect only influences the droplets nearby the surfaces. As the cell gap increases, the bulk droplets are not influenced by the surfaces. During the phase separation processes, the PDLC droplets in the middle layers can still flow and result in larger droplets sizes. Due to the pinning effect of the droplets near surfaces, the morphologies of the cell whose gap is <16 μm are still uniform.

Similar to a conventional PDLC, the light scattering behavior of the thin TN PDLC cell is also independent of light polarization. This is because the orthogonal surface alignments influence the LC orientation in the boundary PDLC layers. This phenomenon of the complementary birefringence colors of the cell is observed under polarized optical microscope when the polarizers are crossed. On the other hand, the PDLC in the thin (d=4 μm) homogeneous cell is dependent on the incident light polarization, as shown in Fig. 7. As the cell gap increases, the surface effect to the bulk LC droplets is reduced due to the longer distance. Therefore, the bulk LC droplets are more randomly distributed and the light scattering behavior is less sensitive to polarization. Also included in Fig. 7 is the voltage-dependent transmittance of a 16-μm homogeneous PDLC cell. Although the cell has the same anchoring energy as the thin cell, the bulk droplets are less ordered in a thicker cell so that the overall light scattering behavior is less dependent on the incident light polarization.

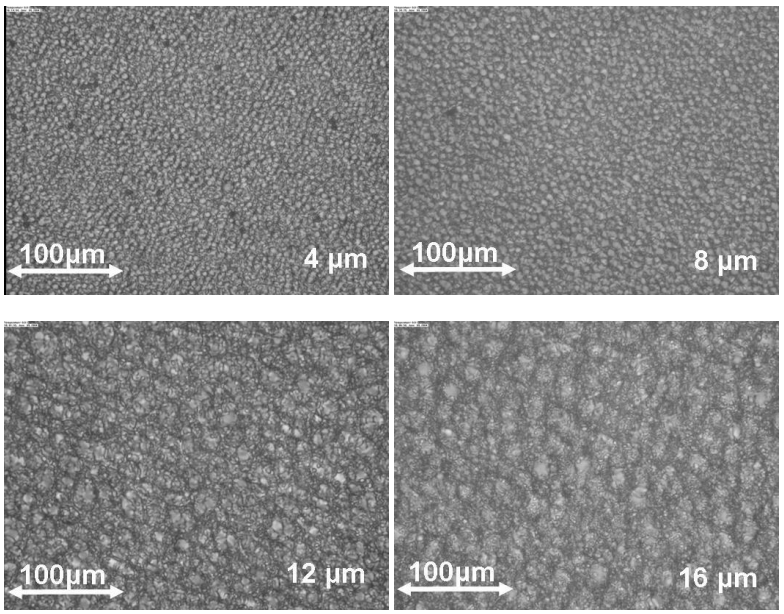

Fig. 6. The morphologies of the homogeneous PDLC cells with various cell gaps at T=20°C observed from a polarized optical microscope. LC/monomer mixture: 70 wt% E48 and 30 wt% NOA65.

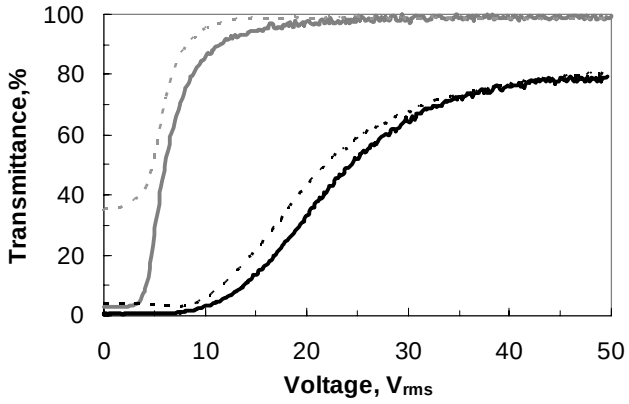

Fig. 7 Voltage-dependent transmittance of the 16-μm (black solid and dashed lines) and 4-μm (gray solid and dashed lines) homogeneous PDLC cells. Solid lines: the input polarization is parallel to the cell rubbing direction. Dashed lines: the input polarization is perpendicular to the rubbing direction. λ=633 nm and T=22°C.

4. CONCLUSION

The surface anchoring effect on the phase separation dynamics of polymer-dispersed liquid crystal with a thin cell gap has been demonstrated. The phase separation dynamics determines the final composite morphology which affects the electro-optic properties of PDLC device. In the conventional PDLC cell without polyimide alignment layers and in the PI cell, the LC droplets flow and coalesce with the neighboring droplets. As a result, the final droplets are larger and size distribution is less uniform. On the

other hand, in the TN and homogeneous cells, the LC droplets are anchored by the strong anchoring force exerted from the surface alignment layers which fix the LC droplets and hinder the coalescence during phase separation. The final morphology in these rubbed cells is much uniform and has smaller droplets.

REFERENCES

1. J. L. Fergason, US Patent 4,435,047 (1984).
2. J. W. Doane, N. A. Vaz, B. G. Wu and S. Zumer, Appl. Phys. Lett. **48**, 269 (1986).
3. N. A. Vaz, G. W. Smith and G. P. Montgomery, Mol. Cryst. Liq. Cryst. **146**, 1 (1987).
4. R. Sutherland, L.V. Natarajan, V.P. Tondiglia and T. J. Bunning, Chem. Mater. **5**, 1533 (1993).
5. F. Basile, F. Bloisi, L. Vicari, and F. Simoni, Phys. Rev. E **48**, 432 (1993).
6. L. Vicari, J. Appl. Phys. **81**, 6612 (1997).
7. S. Matsumoto, M. Houlbert, T. Hayashi, and K. Kubodera, Appl. Phys. Lett, **69**, 1044 (1996).
8. S. X. Cheng, R. K. Bai, Y. F. Zou, and C. Y. Pan, J. Appl. Phys, **80**, 1991 (1996).
9. H. Ren and S. T. Wu, Appl. Phys. Lett. **81**, 3537 (2002).
10. W. J. Chen and S. H. Chen, Phys. Rev. E **52**, 4549 (1995).
11. P. I. C. Teixeira and B. M. Mulder, Phys. Rev. E **53**, 1805 (1996).
12. D. Nwabunma, H. Chiu, and T. Kyu, J. Chem. Phys **113**, 6429 (2000).
13. T. Kyu and H. Chiu, Polymer **42**, 9173 (2001).
14. A. Mertelj, L. Spindler, and M. Copic, Phys. Rev. E **56**, 549 (1997).
15. J. B Nephew, T. C. Nihei, and S. A. Carter, Phys. Rev. Lett. **80**, 3276 (1998)
16. P. S. Drzaic, *Liquid Crystal Dispersions* (World Scientific, Singapore, 1995), Chap. 4.
17. Y. H. Lin, H. Ren, and S. T. Wu, Appl. Phys. Lett. **84**, 4083 (2004).
18. H. M. J. Boot, J. G. Kloosterboer, C. Serbutoviez, and F. J. Touwslager, Macromolecules **29**, 7683 (1996).
19. J. Cognard, Mol. Cryst. Liq. Cryst. Suppl. **1**, 1 (1982).
20. H. Yokoyama and H. A. van Sprang, J. Appl. Phys. **57**, 4520 (1985).
21. S. T. Wu, Phys. Rev. A **33**, 1270 (1986).